**International Journal of Robotics and Automation (IJRA)**
Vol. 5, No. 2, June 2016, pp. 115~135
ISSN: 2089-4856


# Design and Coordination of Cooperative Mobile Robots

**M. Krid, J.C. Fauroux, B.C. Bouzgarrou**
Institut Pascal UMR 6602 UBP/CNRS, Campus Universitaire des Cezeaux, France

**Article Info**

***Article history:***

Received Feb 9, 2016
Revised Apr 28, 2016
Accepted May 14, 2016

***Keyword:***

Cooperative Mobile
Long Payload Ventral
Obstacle Crossing
Robots
Stability Analysis
Stability Criterion
Transportation Mode

**ABSTRACT**

Object transportation is an important task considered in mobile robotics. For many years, it has been performed by single robots, capable to transport payload of moderate size and mass with respect to the robot size and mass. But if the payload gets bigger, the robot fails in the transporting task. For wider or heavier payloads, human operators improve their capacities by working in group. A similar improvement should be expected with a group of mobile robots. In this paper, we proposed a new concept of cooperative mobile robots to deal with the problem of long object transportation in unstructured environment whatever the payload length. The proposed C3Bots AT/VLP robot is formed by the association of two or more mono-robots with simple kinematics forming a polyrobot system. The paper presents several kinematic schemes and the corresponding obstacle-crossing processes. It deals with the problem of how to maintain stable motion for the poly-robot during obstacle crossing. Changes in the internal con_guration of the robot adjust the center of gravity to guarantee stable motion. A speci_c stability criterion for contact on three wheels is presented. By adjusting the relative poses of the front and rear axles with respect to the payload, it is possible to maximize the stability of the poly-robot and its payload during obstacle crossing.



***Corresponding Author:***

Mohamed Krid,
Assistance Professor,
Institut Pascal UMR 6602 UBP/CNRS, Campus Universitaire des Cezeaux,
Les Cezeaux CS 20265, 63175 AUBIERE Cedex, France.
Email: med.krid@gmail.com

## 1. INTRODUCTION

Some tasks are impossible with N robots but possible and easy with N+1 robots [1-3]. The cooperation transport task between two or more robots can be classified in two categories. The first one when the robots have not a mechanical connection. In general this type of robots are used in regular environment [4], [6, 7]. The second one when the robots have a mechanical connection [1], [5], [3]. In this case the robots are used in unstructured environment. We can introduce the term of mono-robot for the single robot and poly-robot for the association of several mono-robots transporting a payload. Using several cooperative mono-robots improves transport capacity and can be helful in many situations such as work in a dangerous environment (radioactiveor or contaminated) or delicate transport (transport of injured people on stretchers). In this case, robots must be able to manoeuvre on irregular grounds and to cross obstacles. Many all-terrain mobile robots were developed for planetary or dangerous area exploration. They have di_erent architectures [8] [3] and locomotion modes [9, 10] but the same purposes: they must be able to evolve on irregular or unstructured environment and to guarantee a minimum stability during a mission. Cooperative mobile robots for transport are often complex. They use many actuated joints and a sophisticated control system. The simpler ones, such as Army Ant cooperative lifting robots [8] have greater facility to comply with numerous constraints on the payload and the environment.

### 1.1. Obstacle-Crossing

Many solutions for obstacle crossing can be found in the literature. We can classify these solutions according to several criteria: locomotion mode, number of actuated joints or controller complexity to achieve the desired mobility. Various locomotion modes can be considered: leg, track and wheel modes. Whereas legged mobile robots ensure a superior adaptability to many kinds of obstacle, their mechanical architecture is complicated because active control algorithms are used[11][12]. Tracked mobile robots provide acceptable mobility in off-road environments by virtue of their wide contact surface with the ground, but excessive friction loss during direction changing also results in poor energy eficiency[13]. Compared to other categories, wheeled mobile robots can be constructed with a simpler structure so that fast movement as well as good energy eficiency are guaranteed without any complicated control strategy [14] [15], but they are limited for obstacle climbing. Some studies combine tracks and legs or wheels and legs to provide new locomotion modes. In [9], legs and tracks are combined and allow the **AZIMUT** robot to climb over obstacles. For the same goal Open **WHEEL** i3R [10] and Rocker [17] mobiles robots combine legs and wheels to provide new hybrid locomotion modes.

### 1.2. Cooperative Robots

Cooperative mobile robots can be classified in two categories according to their cooperation strategy. In the first type, we have one master robot and the rest of the robots follow it. It is the leader-follower cooperation type [18][19]. In the second category, all the robots are equivalent. If the initial states of the robots are exchanged we have two possibilities: All the robots share their information and plan their motion after consultation [20]. Each robot uses only its state to compute its motion autonomously [11]. The cooperation style depends on the type of the task. For example, when two humans transport a payload, if they do not have the same field of vision they need to adopt a leader-follower cooperation. But if they have the same field of vision, it is simpler to use autonomous cooperation.

### 1.3. Payload Transport

Many vehicles used to transport objects can be found in the literature. We can classify these transporters according to their size compared to the size of the payload. The transporter can be smaller than the payload [3][8] or bigger [21]. The payload can have di_erent positions on the vehicle. It can be placed on the top surface[8] or on the bottom surface [21] or even become a part of the structure [22]. The solution presented in [22] is an interesting transport system, comprising a tractive engine and a trailer, which are interconnected by the payload itself during its transport. This kind of solution remains a particular one which is suitable for special needs, such as the transport of large parts (the giant blades of a wind-turbine, in this case). In the literature, cooperative mobile robots for transport are often complex. They use many actuated joints and a sophisticated control system. The simpler ones must comply with many constraints on the payload and the environment, such as Army Ant cooperative lifting robots [8]. In this paper, we design cooperative transporter mobile robots with a minimum number of actuators and a simple controller. Our robot, which is composed of several mono-robots, must be able to fetch a long payload, to transport it over irregular ground and to cross obstacles with it. This concept of collaborative transport allows the robots complexity to be adapted to the shape and mass of the pay-load. A poly-robot with N units will be capable of carrying N times the maximum payload of a single mono-robot. In order to decrease the mass of the connecting parts, it was decided to use the payload as a structural frame between the mono-robots. In this paper, we present the synthesis of the cooperative C3Bots AT/VLP (All-Terrain /Ventral Long Payload) mobile robot. Section 2 describes the resulting poly-robot, associating two or more identical mono-robots that connect directly to the payload for transporting it. Section 3 describe a kinematics of the mono-robot, illustrating the required degrees of freedom for the ventral manipulator. Section 4 presents a method of systematic synthesis of possible equivalent kinematics. In section 5, the mobilities are combined to present two obstacle-crossing modes, where stability is achieved by motions of the mono-robots with respect to the payload. The _rst mode uses only two mono-robots but requires complex control and 3D motions. The second mode uses only 2D motions but requires 3 mono-robots or more. Section 6 present a reduced multi-body model of the ploy-robot that has been built to simulate the crossing operation on MSC-ADAMS software. Section 3 presents an obstacle-crossing process in eighteen stages with only two mono-robots, where stability is achieved by positioning the mono-robots with respect to the payload. In section 4, geometric and kinematic models are presented. These two models will be used in section 5 in order to study the stability of the poly-robot and its payload.

## 2. DESIGN APPROACH

The concept presented in this work is inspired from the OpenWHEEL i3R platform [10]. It uses a similar and extended process for obstacle crossing as the original OpenWHEEL i3R platform but with another kinematics scheme suitable for transporting long payloads. The robot concept was also introduced to bring modularity and simplify robot manufacturing and maintenance, as a defective mono-robot can easily be replaced.

### 2.1. OpenWHEEL i3R Architecture

The main purpose of this paper is to design a ground-based robot able to transport a long payload and to climb obstacles in cooperative mode. A longer robot version was derived from the original OpenWHEEL i3R(Fig.1) and adapted to the considered tasks (Fig.??). Designing mobile robots with the ability to climb obstacles represents an important task for robot designers. One of these archi- tectures is the OpenWHEEL i3R platform [10] with its original climbing process as shown in Fig.1. It contains two axles, linked with a serial inter-axial mechanism using three simple revolute joints (an active central joint for warping and two passive joints for steering). Each axle contains two actuated wheels (Fig.2). The climbing process of the OpenWHEEL i3R platform is a serpentine movement divided into nineteen stages. Each stage corresponds to a joint motion (amovement of a joint or a wheel contact being removed or regained) (Fig.1).

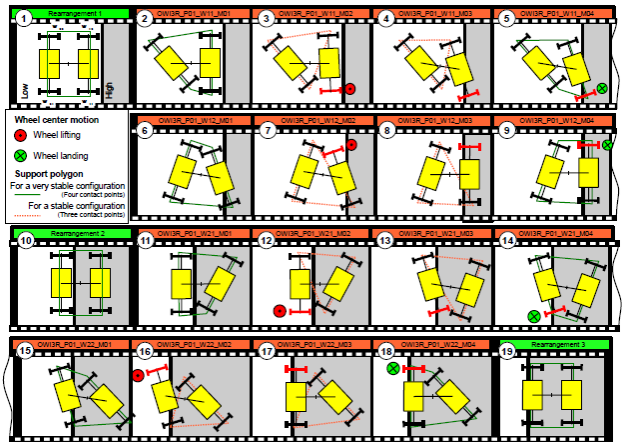


Figure 1. The Climbing Process of the Openwheel I3r Mobile Robot

The stability of the platform is a necessary condition to perform the climbing process. Previous works [23] showed that OpenWHEEL i3R stability during stages 4 - 8 - 13 - 17 of the climbing process (Fig.1) can be maximized if the Wheelbase/Track ratio = 1. At the same time, increasing the Wheelbase/Track ratio improves the pitch stability of the robot when rolling on irregular ground.

### 2.2. Payload Position

The study of the robot stability during the task is important. Before that, the robot kinematic structure should be synthesized, using suitable mobilities sp that stabilization could be possible [24]. Robot stability is evaluated according to developed metrics in literature. Stability margin can be classi_ed in two categories static [25] and dynamic [26] stability margins. This paper only considers low spped mobile robots an uses the static stability margin to compare difeerente structures. Static stability indicators, such as Static Rollover Threshold (SRT) or Static Stability Factor (SSF) [27] rely only on the robot geometric character- istics. In this section, the choice of the position of the gripper mechanism and the payload will be discussed.

To increase the workspace of the robotic system, the robotic manipulator is often put on top of the mobile platform [28][29][30][31]. This location offers high exibility to manipulate the object. But in the case of transport in unstructured environment and obstacle crossing [3][32][11] it will be source of instability, because it increases the height of the center of mass [33] [34] or moves it in an undesirable area [28] [35]. To improve static stability as shown in figures 3 and 4, the gripper will be integrated in the bottom of the robot between the two wheels (left and right). In this case, the grasping task of the payload will be easier as shown in figure 3. The robot should just position itself above the payload. Then,in the case of at ground, the weight of the payload will be shared between left and right side during and after the grasping task as shown in figure 4. The vertical motion of the gripper requires a suitable mobility in the system to elevate the payload (change the height of the total centre of mass of the robot). As a conclusion, the integration of the the gripper at the

bottom of each axle simplifies the payload gripping task and improves stability by decreasing the height of the total centre of mass.

Figure 2. OpenWHEEL i3R

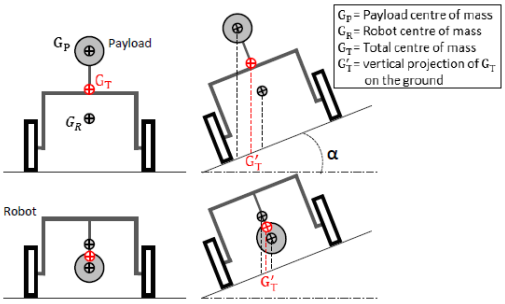


Figure 3. Inuence of the payload position: a lower payload leads to smaller motions of the projected total centre of mass G'T on inclined grounds.

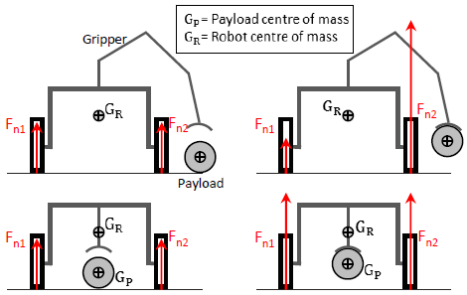


Figure 4. Inuence of the gripper mechanism position: ventral transport decreases roll-over risk.

### 2.3. Functional Requirements for the New Poly-Robot

The first idea is that wheelbase = track is required for the climbing phases and a long wheelbase (wheelbase >> track) for the rolling phases, which means an adjustable wheelbase is needed (functional requirement FR). A second idea led us to separate the initial OpenWHEEL i3R robot into two identical singleaxle mono-robots to improve modularity (requirement R2). Combining these requirements gave rise to the C3Bots AT/VLP (All-Terrain / Long Payloads) robot concept using two single-axle mono-robots that will have to lift the payload, translate along its axis to change the wheelbase length and rotate around the same axis to warp the poly-robot and elevate one wheel with respect to the three others.

1. FR1 Choosing the appropriate number of axles for rolling.
2. FR2 Lifting the payload from the ground.
3. FR3 Handling various type of payloads (unstructured/low sti_ness).
4. FR4 Changing direction.
5. FR5 Climbing obstacles.
6. FR6 Ensuring stability.
7. FR7 Keeping all the wheels in contact on irregular ground.

### 2.4. Mono-Robot Architecture

The transport platform depends on the mono-robot architecture. More specifically, poly-robot mobility depends on the interconnection between all the mono-robots, some of them being redundant.
The mono-robot must be able to roll on the ground (Ry mobility) and lift the payload. It needs a gripping mechanism (gripper) that ensures the connection between the axle frame and the payload. The mono-robot must be able to change its motion direction (using Rz steering mobility) without modifying the payload orientation during transport in order to perform appropriate grasping operations. During the transport mission, each mono-robot must be ableto translate along the payload axis (Tx mobility) and rotate around the same axis (Rx mobility). Rx mobility will also help to keep all the wheels in contact with the irregular terrain. The mono-robot can transport small payloads over at ground by itself . During solo locomotion, stability can be obtained using various solutions:

1. Active pitch control in the same way as [16].
2. Adding a retractable arm with a passive caster wheel.

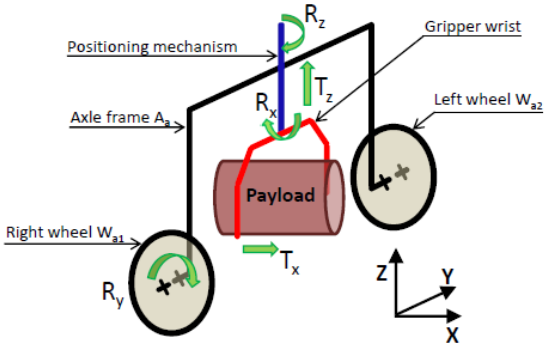


Figure 5. DOF between different bodies of the mono-robot.

## 3. REQUIRED MOBILITIES AND EXAMPLE OF KINEMATICS

The mono-robot includes an axle, a positioning mechanism and a gripping mechanism. One feasible kinematics of the positionning mechanism is presented in Fig.6 and 7. The mono-robot, denoted MRa, includes two wheels Wa1 and Wa2 motorized independently with two motors (with index "a" equals to "1" for frontaxle and "2" for rear axle, "1" for right wheel and "2" for left wheel). To be able to manipulate the object, the robot is equipped with a gripper mounted at the bottom of the chassis. The originality of the concept lays on the kinematic chain of the positioning mechanism. The axle frame (Aa) can freely steer around the cylindrical joint Ca with respect to slider (S1a). The remaining vertical mo- torized translation Tza of Ca allows controlling the altitude of the gripper and consequently of the payload. The roll motion Rxa between the slider body (S1a) and the support body (S2a) is ensured by the revolute motorized joint (Ra3) which is compulsory to reproduce warping motion of one axle roughly around the longitudinal axis of the payload, as the original OpenWHEEL i3R did.

The connection between the mono-robots is ensured by the transported payload as shown in Fig.11. The co-manipulation of the payload by the two mono-robots allows obstacle crossing. The poly-robot combines the mobilities of the mono-robots. It can control the passive rotation Rza of the cylindrical joint (Ca) on each mono-robot by the di_erence of angular velocities of the two wheels of each axle. The redundant revolute joints R13 (front) and R23 (rear) give a warping degree of freedom to the poly-robot. When joints Ra3 are actuated (either R13 or R23), a warping motion is generated of one mono-robot around the joint Ra3 axis with respect to the other mono-robot. This movement allows to lift the exploration wheel off the ground. We have therefore a new configuration of the system with only 3 wheel-ground contacts. Finally, prismatic joint Pa between gripper GWa and support S2a in each mono-robot allows translating the mono-robot along the payload axis. As a conclusion, the implementation shown in Fig.?? provides the four mobilities required on each mono-robot for stable payload transport and obstacle of the poly-robot:

1. a rotation Rxa for wheel elevation on obstacles.
2. a rotation Rza for steering and stabilization on 3 wheels con_guration.
3. a translation Txa for on improved stabilization with a long payload.
4. a translation Tza for payload elevation.

Several equivalent serial kinematic chains are presented in Fig.9 and can be used for a real implementation. The kinematics presented in Fig.6 and Fig.11 allows the poly-robot to transport long payload in a modular

way and also to cross obstacles. Before detailing the crossing modes, the next section will present an exhaustive method to synthesize alternative kinematics.

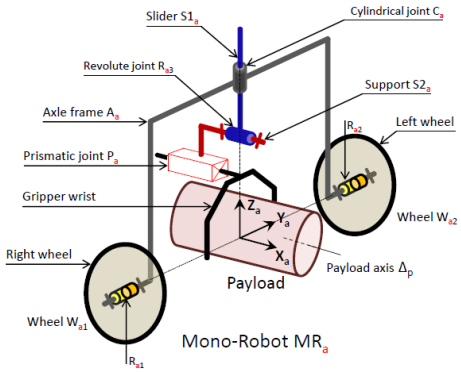


Figure 6. Kinematic diagram of a mono-robot MRa.

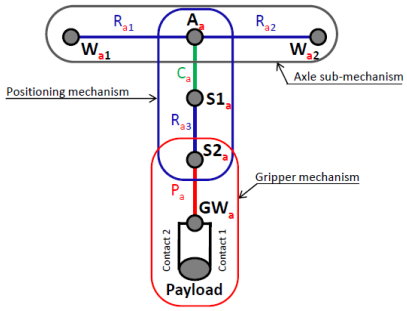


Figure 7. Kinematic graph of a mono-robot MRa.

## 4. SYSTEMATIC SYNTHESIS OF THE POSITIONING MECHANISM

The positioning mechanism is the kinematic chain that connects the axle to the gripper mechanism of the considered mono-robot (Fig. 9). In this work, only serial chains will be considered. The required mobilities of the end of the chain (gripper) with respect to its beginning (axle) are Rx, Rz, Tx and Tz, as found in the previous section. The considered joints will be: the revolute joint R, to provide rotations Rx and Rz; the prismatic joint P to provide translations Tx and Tz; the cylindrical joint C to provide independent rotational and translational motions along a given axis. Helical joint H will not be considered here because of the coupled motions.

The systematic synthesis is based on the enumeration of the non-redundant combinations of R, P and C joints capable to provide the required mobilities Rx, Rz, Tx and Tz. Four cases can be distinguished:

1. Permutations of two joints Cx and Cz;
2. Permutations of three joints Cx, Rz and Pz;
3. Permutations of three joints Cz, Rx and Px;
4. Permutations of four joints Rx, Tx, Rz and Pz.

As the number of permutations of n elements is equal to n!, the total number of potential kinematics is 2! + 3! + 3! + 4! , that is to say a total of 38 possible mechanisms, enumerated in Table 1. However, the _nal solutions have to comply to additional functional requirements, that can be translated into design rules, and that will restrict the combinatorial explosion. In the following lines, the kinematic chains are all oriented from the axle to the gripper. A first requirement is that joints Rx or Cx should serve for warping the axle around the payload axis, in the same way as the OpenWHEEL i3R robot. This means that the orientation of rotation axis of joints Rx or Cx should be kept parallel to the payload axis, unmodified by the kinematic chain that follows these joints. The corresponding design rule R3 is that Rz or Cz joints are forbidden after Rx or Cx joints. Applying R3 to the 38 mechanisms allows to extract 19 solutions (Table 1, column Rule R3). A second requirement is that joints Rz or Cz should serve for axle steering. This means two things :

1. The Rz or Cz rotation axis should be kept perpendicular to the wheel axis. This assertion can be reformulated into the following: the orientation of the axis of rotation of Rz or Cz joint should not be modified by the kinematic chain that precedes these joints. Finally, the design rule R4 appears to be : Rx or Cx are forbidden before Rz or Cz.
2. The Rz or Cz rotation axis should pass through the wheel axis. This requires that the position of the axis of rotation of Rz or Cz joint should not be modi_ed by the kinematic chain that precedes these joints. This can be summarized in a fifth design rule R5: Px or Cx are forbidden before Rz or Cz.

| Description | Solution # | Kinematic chain | Rule R3 | Rule R3 | Rule R5 | Solutions |
|---|---|---|---|---|---|---|
| 2 joints Cx and Cz | S 01 | Cx Cz | | | | |
| | S 02 | Cz Cx | x | x | x | x |
| 3 joints Cx Rz Pz 3!=6 permutations | S 03 | Cx Rz Pz | | | x | |
| | S 04 | Cx Pz Rz | | | | |
| | S 05 | Rz Cx Pz | x | x | x | x |
| | S 06 | Rz Pz Cx | x | x | x | x |
| | S 07 | Pz Cx Rz | | | | |
| | S 08 | Pz Rz Cx | x | x | x | x |
| 3 joints Cz Rx Px 3!=6 permutations | S 09 | Cz Rx Px | x | x | x | x |
| | S 10 | Cz Px Rx | x | x | x | x |
| | S 11 | Rx Cz Px | | | x | |
| | S 12 | Rx Px Cz | | | | |
| | S 13 | Px Cz Rx | x | x | | |
| | S 14 | Px Rx Cz | | | | |
| 4 joints Rx Px Rz Pz 4!=24 permutations | S 15 | Rx Px Rz Pz | | | | |
| | S 16 | Rx Px Pz Rz | | | | |
| | S 17 | Rx Rz Px Pz | | | x | |
| | S 18 | Rx Rz Pz Px | | | x | |
| | S 19 | Rx Pz Px Rz | | | | |
| | S 20 | Rx Pz Rz Px | | | x | |
| | S 21 | Px Rx Rz Pz | | | | |
| | S 22 | Px Rx Pz Rz | | | | |
| | S 23 | Px Rz Rx Pz | x | x | | |
| | S 24 | Px Rz Pz Rx | x | x | | |
| | S 25 | Px Pz Rx Rz | | | | |
| | S 26 | Px Pz Rz Rx | x | x | | |
| | S 27 | Rz Rx Px Pz | x | x | x | x |
| | S 28 | Rz Rx Pz Px | x | x | x | x |
| | S 29 | Rz Px Rx Pz | x | x | x | x |
| | S 30 | Rz Px Pz Rx | x | x | x | x |
| | S 31 | Rz Pz Rx Px | x | x | x | x |
| | S 32 | Rz Pz Px Rx | x | x | x | x |
| | S 33 | Pz Rx Px Rz | | | x | |
| | S 34 | Pz Rx Rz Px | | | x | |
| | S 35 | Pz Px Rx Rz | | | x | |
| | S 36 | Pz Px Rz Rx | x | x | x | x |
| | S 37 | Pz Rz Rx Px | x | x | x | x |
| | S 38 | Pz Rz Px Rx | x | x | x | x |

Figure 8. Enumeration of the 38 permutations using either two joints (Cx, Cz) or three joints (Cx, Rz, Pz) or three joints (Cz, Rx, Px) or four joints (Rx, Px, Rz, Pz) and providing the four independent mobilities Rx, Rz, Tx and Tz.

It appears that rule R4 gives exactly the same solutions as rule R3. This would not be the case if were considered also redundant solutions. The last rule R5 restricts the number of solutions to 22 out of 38 (Table 1, column Rule R5). By keeping only the solutions complying simultaneously to R3, R4 and R5, a final group of 15 solutions can be found. The fifteen final solutions are S02, S05-06, S08 - 10, S27 - 32, S36-38 and are represented in Fig. 9, where can be seen all the generated kinematics. This synthesis method is rather general and could be easily completed with additional design rules, provided that they can be formulated independently from the dimensions of the mechanism and referring only to its qualitative structure.

## 5. PROCESS FOR OBSTACLE CROSSING

C 3Bots AT/VLP can adopt more than one process for obstacle crossing [36]. It can be defined by the number of axle that form the poly-robot. The climbing process with three axles and more is very simple compared to the twoaxle configuration, because during the climbing process the poly-robot has always two axles or more on the ground, and only one axle is lifting off to climb the obstacle (more details in [36]).

Fig.10 represents a view of all phases of the climbing process. Each sub-figure represents the pose of the poly-robot at the end of the 18 climbing phases. Each phase is achieved by the motion of a single joint or by a change in the wheel-ground contacts. By considering different possible configurations for the robot

design, we can state as a general conclusion that the three-axle (and more) design enables an easy 2D obstacle crossing mode at the price of a high number of axles. Hereinafter, we focus on a poly-robot with two mono-robots, since it represents a more attractive design. The associated warping mode described in (Fig.10) will be optimized to maximize stability.

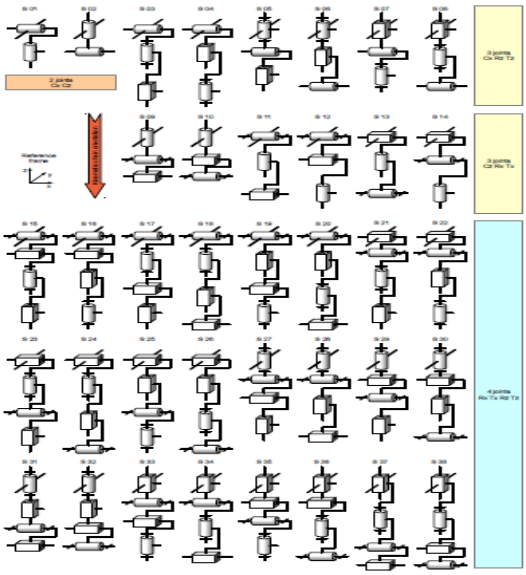

Figure 9. Representation of the 38 kinematics
corresponding to the enumerated joint permutations

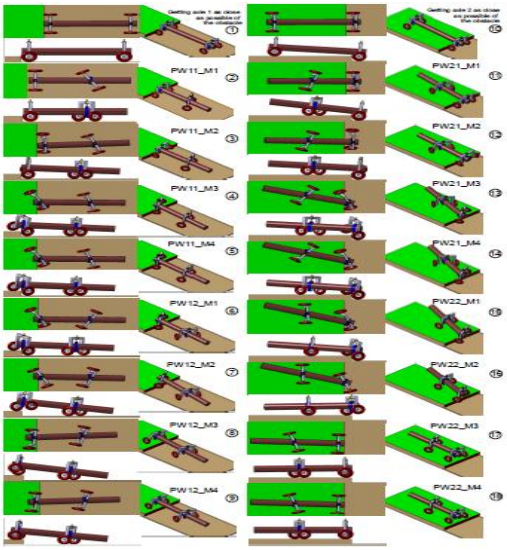


Figure 10. Climbing sequence of the poly-robot with only two axles.

## 6. POLY-ROBOT MODELLING

In this section, geometric and kinematic models are presented. The formulation of these models is performed using the assumption of rolling without slipping at the wheel-ground contacts. With these models, we can de_ne the relation between different geometric variables of the poly-robot. This will be used later in section 7. for the stability analysis of the poly-robot based on an original stability criterion.

### 6.1. Geometric Parameters

This section introduces the geometric parameters of the robot which will be used to evaluate the stability criterion in the next section. Each body of the robot has a local reference frame. $F_{a1}$ and $F_{a2}$ are

respectively the local frames fixed to axle frame Aa and slider S1a . FWa1 and FWa2 are respectively the local frames fixed to the right and left wheels of axle a. The ground reference frame F0 is fixed to the half-width of the rear wheel axles. Fp is the frame fixed to the payload. In order to simplify the expression of the geometric model, the centres of frames F12, F22 and Fp are aligned. The rotations of the frames are given by three rotation variables: θa, βa and ϕa (Fig.11). In this paper we study only the climbing task. We control the revolute joints Ra1;Ra2;Ra3 of each mono-robot, the translation motion of each cylindri- cal joint Ca and prismatic joint Pa. We start by denoting the angular position of each wheel, defined by the rotation angle between the wheel and chassis around Was (Figure12)

$$\beta_{W_{as}} = (\vec{x}_{W_{as}}, \vec{x}_{a1}) = (\vec{z}_{W_{as}}, \vec{z}_{a1}) \quad (1)$$

We denote $I_{as}$ the point of contact between wheel Was and the ground. We denote the yaw (passive cylindrical joint Ca) and roll (active revolute joint Ra3) motions between front and rear mono-robots and the payload by θ1, θ2 and ϕ1, ϕ2 respectively.

$$\theta_a = (\vec{x}_{a1}, \vec{x}_{a2}) = (\vec{y}_{a1}, \vec{y}_{a2}) \quad (2)$$

$$\phi_a = (\vec{y}_p, \vec{y}_{a2}) = (\vec{z}_p, \vec{z}_{a2}) \quad (3)$$

Finally, we denote the pitch motion between the rear mono-robot and the fixed frame $F_0$ by βa.

$$\beta_a = (\vec{x}_0, \vec{x}_{a1}) = (\vec{z}_0, \vec{z}_{a1}) \quad (4)$$

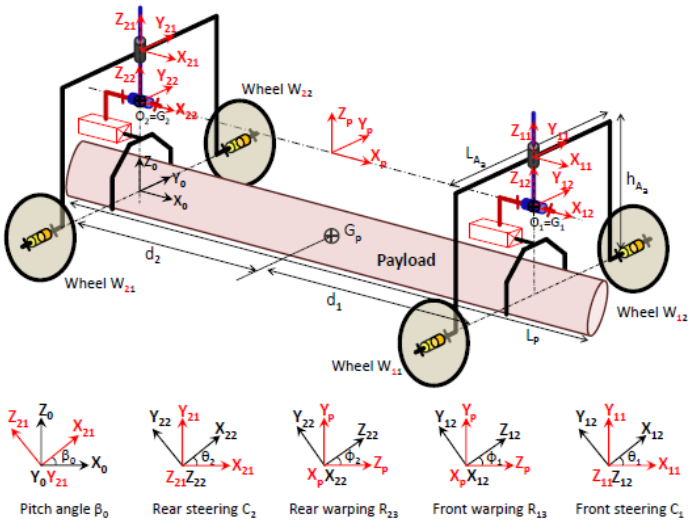


Figure 11. Relative position of each frame and associated angles.

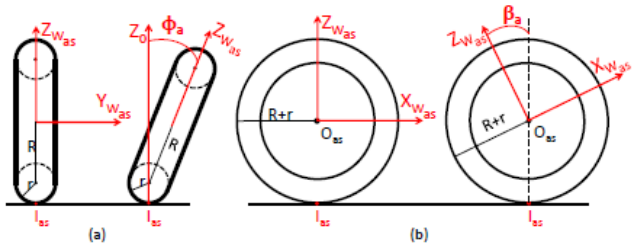


Figure 12. Geometric parameters of the wheel: lateral and longitudinal motion

Mono-robots can translate along the payload. Their relative position is defined by the distance from the c.o.m of the mono-robot MRa to the c.o.m of the payload, denoted da. The cylindrical joint in each mono-robot allows the gripper to translate vertically in order to grasp and adjust the height of the payload. For this

geometric configuration, we define a homogeneous matrix between the frame and the fixed frame of reference F0. Thus the coordinates of the wheelground contact points are expressed in F0 and we can obtain the position of the c.o.m of the poly-robot.

### 6.2. Geometric Model

The aim of the geometric model is to express the relation between the input variables of the poly-robot, which are the warping angles ϕ1; ϕ2, and the output variables βa; θ1; θ2. We start by deFIning the coordinates of each contact point Ias in the local frame FWas ; we obtain the displacement of the contact point under the assumption of rolling without slipping and the position of the centre of mass expressed in the reference frame F0.

#### 6.2.1. Coordinates Of Wheel Contact Points

Each mono-robot is assumed to have torus-shaped wheels, which leads us to consider two radii, R and r (Figure 12). The rolling wheel radius can be approximated by Rw = R + r. We de_ne the 'exploring axle' as the axle that contains the exploring wheel, while the other axle is referred to as the 'supporting axle'. The contact point is the intersection of the external surface of the wheel with the ground and it depends on the position of the vehicles and the value of the roll and the pitch angles of axles (ϕa and βa). The exploring wheel only has contact with the ground in stages M01 and M04. The other wheel of the exploring axle always remains in contact with the ground. As shown in Figure 12-a, the contact point Ias is de_ned in the wheel frame by:

$$I_{as} = \begin{pmatrix} 0 \\ r\sin\phi_a \\ -(R + r\cos\phi_a) \end{pmatrix}_{FW_{as}} \tag{5}$$

For the supporting axle, the wheels are connected to the legs by actu- ated revolute joints which are locked, so the pitch angle will also have an action on the wheels by a rear movement. The wheels will have a rolling motion of the pitch angle βa coupled with a rear translation, and as shown in Figure 12-b, the contact point will be expressed in the wheel frame as:

$$I_{as} = \begin{pmatrix} -R_w\sin\beta_a \\ 0 \\ -R_w\cos\beta_a \end{pmatrix}_{FW_{as}} \tag{6}$$

#### 6.2.2. Rolling Without Slipping

In the case for rolling without slipping, the position, velocity and acceleration of the centre of mass are directly related to the rolling angle of rotation, the angular velocity, and the angular acceleration of the wheel. Two rigid bodies in contact, assuming rolling without slipping, have a zero relative speed at their point of contact. Thus we can write:

$$\begin{cases} \vec{V}_{O_{as}\in W_{as}/F_0} = \begin{pmatrix} \dot{X} \\ \dot{Y} \\ 0 \end{pmatrix}_{F_0} \\ \vec{V}_{I_{as}\in W_{as}/F_0} = 0 \end{cases} \tag{7}$$

$$\vec{V}_{O_{as}\in W_{as}/F_0} = \vec{V}_{I_{as}\in W_{as}/F_0} + \overrightarrow{O_{as}I_{as}} \wedge \vec{\Omega}_{W_{as}/F_0} \tag{8}$$

with

$$\Omega_{W_{as}} = \begin{pmatrix} \dot{\phi}_a \\ \dot{\beta}_a \\ 0 \end{pmatrix}_{F_0} \tag{9}$$

and the following exspression

$$\begin{cases} \dot{X} = \dot{\beta}_a R_w \\ \dot{Y} = r\dot{\phi}_a \end{cases} \tag{10}$$

We deduce by integration of the kinematic relations (10) the coordinate variation of the contact points of the supporting and exploring axles:

$$\begin{cases} X_{t_m} = X_{t_{m-1}} + \Delta\beta_a R_w \\ Y_{t_m} = Y_{t_{m-1}} + r\Delta\phi_a \end{cases} \quad (11)$$

To deduce the di_erent variables of the poly-robot (β2; θ1; θ2) we compare the coordinates of the contact points Ias at t2, the beginning of the warping motion and t3, the end of the motion. Similar calculation can be performed during all the warping manoeuvres PWas□M2 (stage 3,7,12,16). This information can be found in the annex.

### 6.2.3. Coordinates of the Centre of Mass

In order to determine the c.o.m coordinates of the poly-robot, we first have to define the masses of each part of the robot. We suppose that each mono-robot MRa has the same mass ma, and we denote mp the mass of the payload. After defining the masses, we also define the centre of mass position (c.o.m) of each axle. We denote G the c.o.m of the poly-robot, and it is defined in the reference frame F0 in equation 12 as follows:

$$\overrightarrow{OG} = \frac{m_a\left(\overrightarrow{OG_1} + \overrightarrow{OG_2}\right) + m_p\overrightarrow{OG_p}}{2m_a + m_p} \quad (12)$$

The centre of mass of the front and rear mono-robots and the payload G1;G2;Gp respectively coincides with the origin of the frame related to each body. We have to express the coordinates of each point in the frame of reference *F*0.

$$\overrightarrow{O_1G_1} = \begin{pmatrix} 0 \\ 0 \\ 0 \end{pmatrix}_{F_{12}}, \overrightarrow{O_2G_2} = \begin{pmatrix} 0 \\ 0 \\ 0 \end{pmatrix}_{F_{22}}, \overrightarrow{O_pG_p} = \begin{pmatrix} 0 \\ 0 \\ z_{G_p} \end{pmatrix}_{F_p}$$

The evaluation of the coordinates of the contact points and c.o.m was implemented using the symbolic calculus software Maxima. Maxima is a symbolicbased mathematical software providing a number of functions for algebraic manipulation, calculus operations, matrix and linear algebra, and other mathematical calculations. We determine the expression of the c.o.m coordinates in the $F_0$ frame using the following formula:

$$G = \frac{1}{m_t}\begin{pmatrix} \begin{pmatrix} \beta_0\left(R+r\right) + h_e\sin\beta_0 + \sin\beta_0\left(d_1 m_a \sin\phi_1 \sin\theta_1 + z_{G_p} m_1\right) \\ +\cos\beta_0\left(d_2 m_p\cos\theta_2 + m_a\left(d_2\cos\theta_2\left(1+\cos\theta_1\right) - d_1\cos\phi_1\sin\theta_1\sin\theta_2\right)\right) \end{pmatrix} \\ m_a\left(-d_1\cos\phi_1\sin\theta_1\cos\theta_2 - d_2\sin\theta_2\left(1+\cos\theta_1\right)\right) - d_2 m_p\sin\theta_2 \\ \begin{pmatrix} \left(R+r\right) + h_e\cos\beta_0 + \cos\beta_0\left(d_1 m_a\sin\phi_1\sin\theta_1 + z_{G_p} m_1\right) \\ -\sin\beta_0\left(d_2 m_p\cos\theta_2 + m_a\left(d_1\cos\phi_1\left(\cos\theta_2 - \sin\theta_2\sin\theta_1\right) + d_2\cos\theta_2\right)\right) \end{pmatrix} \end{pmatrix}_{F_0} \quad (13)$$

## 7. STABILITY ANALYSIS OF A POLY-ROBOT COMPRISING TWO MONO-ROBOTS

The poly-robot is designed to roll in an irregular environment and to cross obstacles. The robot's stability has to be evaluated and guaranteed during climbing tasks. The C 3Bots AT/VLP robot uses low-speed locomotion, so we can neglect its dynamics. The platform is always stable on four wheels since it has a slow motion. The stability issue manifests itself in climbing stages where only three wheels are in contact with the ground. In order to monitor the climbing process, a suitable stability indicator or stability margin has been introduced.

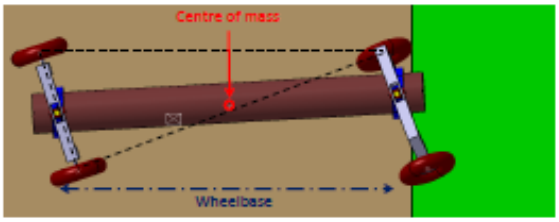


Figure 13. Unstable conFIguration due to the Centre of mass location on the edge of the support triangle of three contact points.

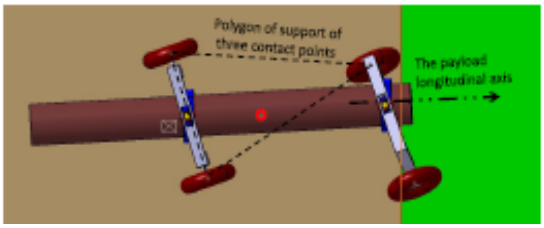


Figure 14. Improvement of stability thanks to the translation of the rear mono-robot along the longitudinal payload axis.

### 7.1. Stability Criterion

The stability margin or indicator cannot depend only on the dimensions of the robot, but also on the wheel-ground contact forces with respect to static equilibrium conditions. After having analysed several existing stability margins in the literature, the indicator which best ful_ls the criterion is Lateral Load Transfer (LLT) [14]. However, it concerns lateral roll-over and supposes that the four wheels of the vehicle are in contact with the ground. Therefore, in order to analyse stability in our case, we propose a new stability criterion that we call the "Tripod Load Transfer" (TLT). This new criterion is based on the evaluation of the contact forces at each contact point between the vehicle and the ground. To this end, three contact points Ic are de_ned with c = 1; 2; 3 and the contact forces at each contact point are denoted Nc. We denote P the gravitational force at the centre of mass G (Fig.15). The vehicle is then stable when all contact forces Nc are greater than zero Nc > 0. A null or negative contact force means that the corresponding wheel is no longer in contact with the ground, which may cause the vehicle to tip over. A TLT stability margin equal to 1 means that the weight of the robot is distributed evenly on the three contact points. In this case the TLT criterion is at its maximum. We determine the Tripod Load Transfer (TLT) using the following formula:

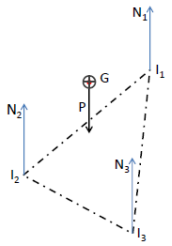


Figure 15. Support polygon for three contact points

$$TLT = \prod_{c=1}^{3} \frac{\left\|\vec{N}_c\right\|}{\|P/3\|} \tag{14}$$

The static equilibrium condition can be expressed as follows:

$$\sum_{c=1}^{3} N_c = \vec{0} \tag{15}$$

$$\sum_{c=1}^{3} M_c = \vec{0} \tag{16}$$

with

$$\vec{M}_c = \vec{N}_c \wedge \vec{G}I_c$$

We define the components of contact forces Ni and the gravitational force P as follows:

$$\vec{N}_c = \begin{pmatrix} 0 \\ 0 \\ N_{zc} \end{pmatrix}_{F_0}, \vec{P} = \begin{pmatrix} 0 \\ 0 \\ -P \end{pmatrix}_{F_0}$$

and GIc represents the vectors joining the centre of mass (c.o.m) G of the poly-robot to the contact points Ic:

$$GI_c = \begin{pmatrix} x_c \\ y_c \\ z_c \end{pmatrix}_{F_0}$$

while equations 15 and 16 give:

$$\begin{cases} \vec{N}_1 + \vec{N}_2 + \vec{N}_3 + \vec{P} = \vec{0} \\ M_1 + M_2 + M_3 = 0 \\ N_{z_c} \geq 0, \forall c \in \{1,2,3\} \end{cases} \quad (17)$$

so we will have the following system to resolve in Nzc

$$\begin{cases} \begin{pmatrix} 1 & 1 & 1 \\ y_1 & y_2 & y_3 \\ -x_1 & -x_2 & -x_3 \end{pmatrix} \begin{pmatrix} N_{z1} \\ N_{z2} \\ N_{z3} \end{pmatrix} = \begin{pmatrix} \vec{P} \\ 0 \\ 0 \end{pmatrix} \\ N_{z_c} \geq 0, \forall c \in \{1,2,3\}. \end{cases} \quad (18)$$

The vehicle is then stable when all contact forces ~Nzc are positively oriented. A non-positive contact force means that the wheel is no longer in contact with the ground, which leads to TLT = 0 (or negative). On the other hand, in ideal conditions when the system is in equilibrium on an horizontal plane with evenly distributed contact forces, each contact force k~Nzck is equal to k ~P=3k and then TLT = 1. We can then write, for a stable configuration:

$$0 < TLT < 1 \quad (19)$$

### 7.2. Stability Analysis During Obstacle Crossing

This section presents the method used to optimize the robot configuration during the climbing process, based on the proposed stability criterion. The op- timization task for this work was explained in algorithm 1. During obstacle crossing, there are various parameters that a_ect the stability of the system. The three important variables for each mono-robot are the warping angle _a, the steering angle _a and the distance between the mono-robots MRa and the centre of mass of the payload da. We de_ne the position of the mono-robot by _ = 2 _ da=Lp.

The stability criterion presented in eq.14 depends on di_erent parameters of the poly-robot (track, obstacle height, masses, . . . ) and variables (relative position of the mono-robots, steering angles, warping angle). The warpingangle depends on the obstacle height, so it is considered as a parameter in the algorithm and varies within [_; _h]. Therefore, it interesting to _nd the postural variables (da; _a) that maximise the TLT criterion.

The considered optimization con_guration variables are the steering angles and distance between the c.o.m of the payload and the mono-robot. The warping angles are considered as a variable input.

The variables (da; _a) which maximise the stability criterion at different warping angles are determined o_-line. To _nd the optimal con_guration, we calculate the surface of the TLT function (da; _a) at di_erent exploring wheel positions or warping angle _ values (see Fig.18 and 19). Then di_erent values of (da; _a) that maximise TLT are recorded for each warping angle _1. Finally, the evolution of the stability criterion is plotted during the warping phase at different (da; _a) (see Fig.20).

The different characteristics of the virtual C 3Bots AT/VLP (All-Terrain/Ventral Long Payloads) are listed in Table 1.

Detect $h_s$ and define the corresponding final warping angle $\phi_{h_s}$
**if** *Stage of the obstacle-crossing process* $= 1$ *or* $6$ **then**
  Maximise $TLT(d_2, \theta_2)$ for the initial $\xi$ and final $\phi_{h_s}$ warping angle
  $TLT_{(d_{2op}, \theta_{2op})} = Min[TLT_{Max}(d_2, \theta_2, \xi), TLT_{Max}(d_2, \theta_2, \phi_{h_s})]$
**end**
**if** *Stage of the obstacle-crossing process* $= 9$ *or* $13$ **then**
  Maximise $TLT(d_1, \theta_1)$ for the initial $\xi$ and final $\phi_{h_s}$ warping angle
  $TLT_{(d_{1op}, \theta_{1op})} = Min[TLT_{Max}(d_1, \theta_1, \xi), TLT_{Max}(d_1, \theta_1, \phi_h)]$
**end**

Algorithm 1. Applied Optimization Loops

| $L_{A_a}$ | $L_p$ | $m_a$ | $m_p$ | $R$ | $r$ | $h_s$ | $h_e$ | $\phi_h$ | $\xi$ |
|---|---|---|---|---|---|---|---|---|---|
| $1,2m$ | $4m$ | $100kg$ | $400kg$ | $0,2m$ | $0,1m$ | $0,3m$ | $0,84m$ | $20°$ | $1°$ |

Table 1. List of geometric parameters

### 7.3. Obstacle-Crossing Strategy

For each phase of the climbing process, the warping angle is de_ned by the crossing task. To _nd the optimal con_guration of the robot ( _a and da), two warping angle are considered (_, a small angle that defines the initial warping angle and _hs , which de_nes the _nal warping angle). Fig.16 and Fig.17

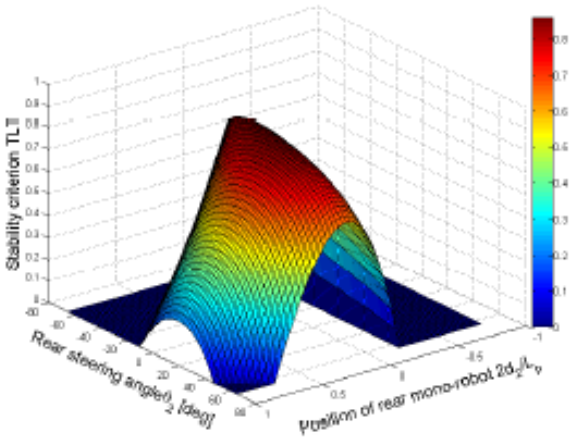


Figure 16. Variation in stability margins with respect to rear axle position for phase 1 with $\phi_1 = \xi$.

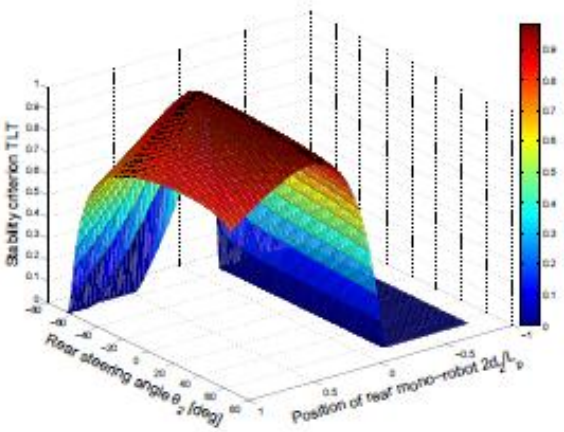


Figure 17. Variation in stability margins with respect to rear axle position for phase 1 with $\phi_1 = \phi_{h_s}$.

The TLT values and the corresponding con_guration (da; _a) are de- duced for each warping angle (one optimal con_guration for each warping angle). During the crossing process (da; _a) can not be changed, so we need to _x these two parameters before starting the climbing process. In _gure 20, the trajectory of the TLT during crossing process (_1 within [1; 15]) is plotted for di_erent optimal con_gurations. In our case the con_guration (da; _a)_=10 was selected for the following reasons: _rst, we chose the most stable con_gurations for the _nal warping angle because it is the position corresponding to the crossing ma- noeuvre ((da; _a)_=10,(da; _a)_=15 and (da; _a)_=20); second, because it has an acceptable TLT value at the initial warping angle (TLT = 0:83), better than the blue and magenta curves ((da; _a)_=20, (da; _a)_=15 respectively). It also has a good TLT value for the _nal warping angle (TLT = 0:945), similar to the blue and magenta curves.

**Discussion of the results**

1. The maximum TLT criterion value for all the _gures is below the value 1, which con_rms the theoretical result given in eq.14. On the other hand, we can note some values of the stability criterion that are null; these values are explained by the fact that the system is unstable in those con_gurations.
2. For the _gures that represent the variation in the stability criterion de- pending on the position of the rear mono-robot, we can notice that the e_ect of the steering angle on the stability criterion is maximum if we take small variations in the steering angle. This result con_rms the observation resulting from the _gures (14) and (13)
3. If we compare the inuence of _ = 2da=Lp (which represents the wheel- base) with the steering angle, we can deduce that the former is more important. In _gure 19 we can deduce that a small interval for _ ensures the stability of the robot (see the horizontal line in _gures (19) and (18)) but the robot is stable on a large interval of _2 (see the vertical line in the _gures).
4. The variation in the warping angle signi_cantly inuences the stability criterion. This inuence is illustrated by _g.16 and _g.17 at warping angles equal to 1_ and 20_ respectively.

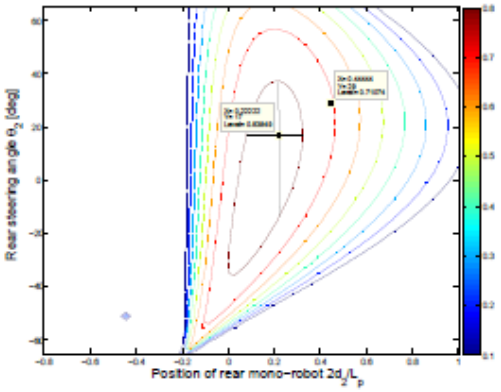


Figure 18. Variation in stability margins in 2D for phase 1 with $\phi_1 = \xi$.

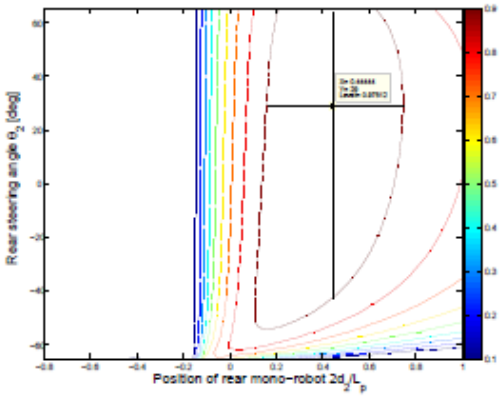


Figure 19. Variation in stability margins in 2D for phase 1 with $\phi_1 = \phi_{h_s}$.

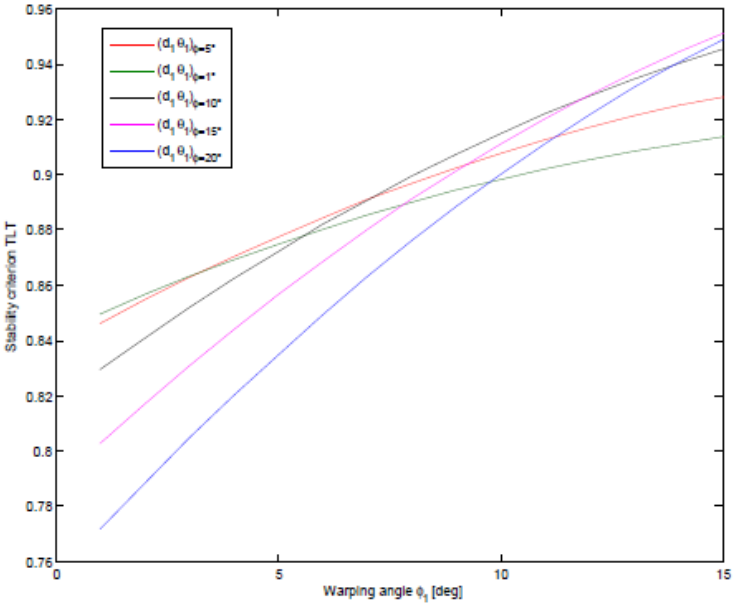


Figure 20. Variation in stability margins during wheel warping for different optimal con_gurations (da; _a)

## 8. SIMULATION RESULTS

In order to verify the proposed strategy for the obstacle crossing, especially regarding stability, a reduced multi-body model of the ploy-robot has been built to simulate the crossing operation on MSC-ADAMS software (Figure 21). Contact forces have been defined between the ground and the wheels. Simulation results show that no tilting or loss of control occur during this operation. Stability condition can be verified by considering ground contact forces.

In fact, the best stability condition is obtained when the normal contact forces of the wheels in contact with the ground are equal. When a normal contact force is close to zero, it can prevent for an eminent lifting of the wheel with a possible tilting of the poly-robot. Hence, a stability margin indicator can be derived from the normal contact forces. In addition, one can define a control strategy or a trajectory planning based on direct measuring or the estimation of the contact forces. The curves in show the evolution of the normal contact forces along the crossing process stages. These forces remain positive for the 3 wheels in contact with the ground, which con_rms the stability of the proposed strategy for the obstacle crossing.

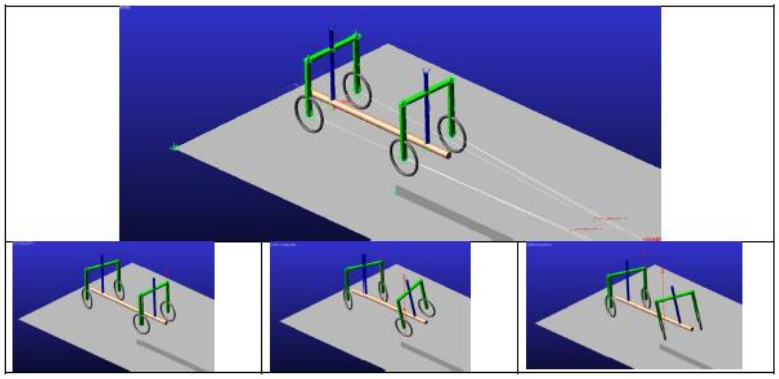

Figure 21. ADAMS model of the poly-robot

## 9. CONCLUSION

In this paper, we proposed a new cooperative mobile robot concept to deal with the problem of long object transportation in unstructured environments, whatever the payload length [37]. The proposed C 3Bots AT/VLP robot is formed by the association of two or more mono-robots with simple kinematics, forming a poly-robot system. This composition of the system gives various advantages, such as the security of the payload and the adaptability of the poly-robot to di_erent sizes and weights of the transported object. This modular architecture enables two modes of obstacle crossing through di_erent stages for each mode. The "warping" mode is used by a con_guration of only two mono- robots. This "2 □ axle" robot con_guration comes at the price of complex control. Meanwhile, the second mode, which can be referred to as the "3□axle" (or more) crossing mode, has simpler control but generates a complex form for the robot, a heavier weight and, ultimately, a more expensive system.

On the other hand, the con_gurations using the warping "2 □ axle" crossing mode require a deeper analysis to determine their stability. During the process, it was noticed that there are few stages where stability is critical. These stages are when the system is moving on only three contact points. To quantify the stability of the system, a new "TLT" static stability criterion was introduced. The stability study showed the usefulness of making the wheelbase variable between the front and rear axles. This allows an optimal distribution of the total weight of the robot over three contact points instead of two, and ensures overall robot/payload stability. This study results in the optimal joint parameters that maximize the stability criterion for a given obstacle geometry.

As a perspective for this work, the optimization of the process for each step and an evaluation of dynamic stability for critical con_gurations of the robots are envisageable. This could be done to ensure a smooth transition between process stages at higher speeds. Finally, the study of the stability of the payload and its position control allows C 3Bots AT/VLP to transport sensitive payloads such as victims or hazardous material that must be maintained in a well-defined position.

**ACKNOWLEDGEMENT**

LabEx IMobS3 Innovative Mobility: Smart and Sustainable Solutions, the French National Centre for Scientific Research (CNRS), Auvergne Regional Council and the European fund for regional development (FEDER) are gratefully acknowl- edged. This work was sponsored by the French government research program "Investissements d'avenir" through the RobotEx Equipment of Excellence (ANR-10-EQPX-44), by the European Union through the Regional competitiveness and employment program 2007 □ 2013 (ERDF Auvergne Region), by French Institute for Advanced Mechanics and by the Auvergne Region.

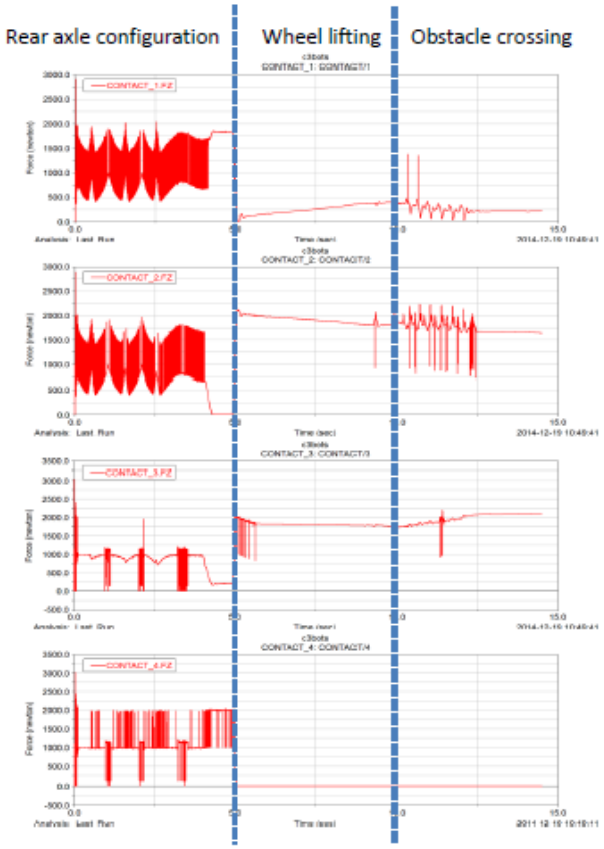


Figure 22. Normal contact forces along obstacle crossing stages

**ANNEXES**

The expression of the contact pointsIascoordinate after starting warping assuming rolling without slipping (3 contact points with the ground):

$$I_{11} = indefinite$$

$$I_{12} = \begin{pmatrix} d_1 + d_2 \\ e + r\phi_1 \\ -(R+r) \end{pmatrix}_{F_0}$$

$$I_{21} = \begin{pmatrix} \beta_0 (R+r) \\ -e \\ -(R+r) \end{pmatrix}_{F_0}$$

$$I_{21} = \begin{pmatrix} \beta_0 (R+r) \\ e \\ -(R+r) \end{pmatrix}_{F_0}$$

The expression of the contact point Iascoordinate after starting warping using the geometric model(3 contact points with the ground):

$$I_{11} = \begin{pmatrix} R\begin{pmatrix} -\cos\beta_0 \sin\phi_1 \sin\theta_1 - \sin\beta_0 \cos\phi_1 + \beta_0) + \sin\theta_1 (-d_1 + \cos\theta_2 (-r\cos\beta_0 \cos\phi_1 \sin\theta_1) + d_1 \sin\beta_0 \sin\phi_1) \\ + \cos\theta_1 \left(\sin\theta_2 (-r\cos\beta_0 \cos\phi_1 \sin\phi_1 - e\cos\beta_0 \cos\phi_1) + d_1 \cos\beta_0 + r\sin\beta_0 \sin^2\phi_1 + e\sin\beta_0 \sin\phi_1\right) \\ +\sin\theta_2 (-r\cos\beta_0 \cos\phi_1 \sin\phi_1 - h_e \cos\beta_0 \sin\phi_1) + d_2 \cos\beta_0 \cos\theta_2 + r(\beta_0 - \sin\beta_0 \cos^2\phi_1) - h_e \sin\beta_0 \cos\phi_1 + h_e \sin\beta_0 \end{pmatrix} \\ \begin{pmatrix} -R + \sin\theta_1 (\sin\theta_2 (e + r\sin\phi_1) - d_1 \cos\phi_1 \cos\theta_2) + \cos\theta_1 (\cos\theta_2 (-e\cos\phi_1 - r\cos\phi_1 \sin\phi_1) - d_1 \sin\theta_2) \\ + \cos\theta_2 (-r\cos\phi_1 \sin\phi_1 - h_e \sin\phi_1) \end{pmatrix} \\ \begin{pmatrix} R(\sin\beta_0 \sin\phi_1 \sin\theta_2 - \cos\beta_0 \cos\phi_1 + 1) + \sin\theta_1 (d_1 \sin\beta_0 \cos\phi_1 \sin\theta_2 + \cos\theta_2 \sin\beta_0 (r\sin\phi_1 + e) + d_1 \sin\beta_0 \cos\phi_1 \sin\theta_2) \\ + \cos\theta_1 \left(\sin\theta_2 \sin\beta_0 \sin\phi_1 (r\cos\phi_1 + h_e) - d_1 \sin\beta_0 \cos\theta_2 + r\cos\beta_0 \sin^2\phi_1 + e\cos\beta_0 \sin\phi_1\right) \\ +\sin\theta_1 \sin\phi_1 \sin\beta_0 (r\cos\phi_1 + h_e) - d_2 \sin\beta_0 \cos\theta_2 + r(1 - \cos\beta_0 \cos^2\phi_1) + h_e \cos\phi_1 (1 - \cos\beta_0) \end{pmatrix} \end{pmatrix}_{F_0}$$

$$I_{12} = \begin{pmatrix} R\begin{pmatrix} -\cos\beta_0 \sin\phi_1 \sin\theta_1 - \sin\beta_0 \cos\phi_1 + \beta_0) + \sin\theta_1 (-d_1 + \cos\theta_2 (-r\cos\beta_0 \cos\phi_1 \sin\theta_1) + d_1 \sin\beta_0 \sin\phi_1) \\ + \cos\theta_1 \left(\sin\theta_2 (-r\cos\beta_0 \cos\phi_1 \sin\phi_1 + e\cos\beta_0 \cos\phi_1) + d_1 \cos\beta_0 + r\sin\beta_0 \sin^2\phi_1 - e\sin\beta_0 \sin\phi_1\right) \\ +\sin\theta_2 (-r\cos\beta_0 \cos\phi_1 \sin\phi_1 - h_e \cos\beta_0 \sin\phi_1) + d_2 \cos\beta_0 \cos\theta_2 + r(\beta_0 - \sin\beta_0 \cos^2\phi_1) - h_e \sin\beta_0 \cos\phi_1 + h_e \sin\beta_0 \end{pmatrix} \\ \begin{pmatrix} -R + \sin\theta_1 (\sin\theta_2 (-e + r\sin\phi_1) - d_1 \cos\phi_1 \cos\theta_2) + \cos\theta_1 (\cos\theta_2 (e\cos\phi_1 - r\cos\phi_1 \sin\phi_1) - d_1 \sin\theta_2) \\ + \cos\theta_2 (-r\cos\phi_1 \sin\phi_1 - h_e \sin\phi_1) \end{pmatrix} \\ \begin{pmatrix} R(\sin\beta_0 \sin\phi_1 \sin\theta_2 - \cos\beta_0 \cos\phi_1 + 1) + \sin\theta_1 (d_1 \sin\beta_0 \cos\phi_1 \sin\theta_2 + \cos\theta_2 \sin\beta_0 (r\sin\phi_1 - e) + d_1 \sin\beta_0 \cos\phi_1 \sin\theta_2) \\ + \cos\theta_1 \left(\sin\theta_2 \sin\beta_0 \sin\phi_1 (r\cos\phi_1 + h_e) - d_1 \sin\beta_0 \cos\theta_2 + r\cos\beta_0 \sin^2\phi_1 - e\cos\beta_0 \sin\phi_1\right) \\ +\sin\theta_1 \sin\phi_1 \sin\beta_0 (r\cos\phi_1 + h_e) - d_2 \sin\beta_0 \cos\theta_2 + r(1 - \cos\beta_0 \cos^2\phi_1) + h_e \cos\phi_1 (1 - \cos\beta_0) \end{pmatrix} \end{pmatrix}_{F_0}$$

$$I_{21} = \begin{pmatrix} \beta_0 (R + r) \\ -e \\ -(R + r) \end{pmatrix}_{F_0}$$

$$I_{21} = \begin{pmatrix} \beta_0 (R + r) \\ e \\ -(R + r) \end{pmatrix}_{F_0}$$

The expression of the c.o.m coordinate after starting warping using the geometric model in the fixed frame *F*0

$$G = \frac{1}{m_t} \begin{pmatrix} \beta_0 (R+r) + h_e \sin\beta_0 + \sin\beta_0 \left(d_1 m_a \sin\phi_1 \sin\theta_1 + z_{G_p} m_1\right) \\ + \cos\beta_0 \left(d_2 m_p \cos\theta_2 + m_a \left(d_2 \cos\theta_2 \left(1+\cos\theta_1\right) - d_1 \cos\phi_1 \sin\theta_1 \sin\theta_2\right)\right) \\ m_a \left(-d_1 \cos\phi_1 \sin\theta_1 \cos\theta_2 - d_2 \sin\theta_2 \left(1+\cos\theta_1\right)\right) - d_2 m_p \sin\theta_2 \\ (R+r) + h_e \cos\beta_0 + \cos\beta_0 \left(d_1 m_a \sin\phi_1 \sin\theta_1 + z_{G_p} m_1\right) \\ - \sin\beta_0 \left(d_2 m_p \cos\theta_2 + m_a \left(d_1 \cos\phi_1 \left(\cos\theta_2 - \sin\theta_2 \sin\theta_1\right) + d_2 \cos\theta_2\right)\right) \end{pmatrix}_{F_0}$$

**REFERENCES**


[1] Hara, M., Fukuda, M., Nishibayashi, H., Aiyama, Y., Ota, J., Arai, T.: Motion control of cooperative transportation system by quadruped robots based on vibration model in walking. *IEEE/RSJ International Conference Intelligent Robots and Systems*, IROS 1999. on, vol. 3, pp. 1651{1656.

[2] Mellinger, D., Shomin, M., Michael, N., Kumar, V.: Cooperative grasping and transport using multiple quadrotors. Distributed Autonomous Robotic Systems 2013, Springer Tracts in Advanced Robotics, vol. 83, pp. 545{558.

[3] Trebi-Ollennu, A., al: Mars rover pair cooperatively transporting a long payload. *IEEE International Conference Robotics and Automation*, ICRA 2002. pp.3136{3141.

[4] Fujii, M., Inamura, W., Murakami, H., Tanaka, K., Kosuge, K.: Cooperative control of multiple mobile robots transporting a single object with loose han- dling. *IEEE International Conference Robotics and Biomimetics*, ROBIO 2007. pp. 816{822.

[5] Yamaguchi, H.: A distributed motion coordination strategy for multiple nonholonomic mobile robots in cooperative hunting operations. Robotics and Autonomous Systems 2003.43(4), pp. 257 { 282 .

[6] Loh, C.C., Trachtler, A.: Laser-sintered platform with optical sensor for a mobile robot used in cooperative load transport. 37th Annual Conference on *IEEE Industrial Electronics Society* IECON 2011. pp. 203{208.

[7] Johnson, P., Bay, J.: Distributed control of simulated autonomous mo- bile robot collectives in payload transportation. Autonomous Robots 1995. pp.43{63.

[8] Bay, J.: Design of the army-ant cooperative lifting robot. *IEEE Robotics Automation Magazine* 1995. pp. 36{43.

[9] Michaud, F., al: Co-design of azimut, a multi-modal robotic platform. IEEE/RSJ International Conference Intelligent Robots and Systems, IROS 2003. on, vol. 3, pp.2553{2558.

[10] Fauroux, J.C., Chapelle, F., Bouzgarrou, B.: A new principle for climbing wheeled robots: Serpentine climbing with the open wheel platform. *IEEE/RSJ International Conference Intelligent Robots and Systems*, IROS 2006. pp. 3405{3410.

[11] Aiyama, Y., Hara, M., Yabuki, T., Ota, J., Arai, T.: Cooperative trans- portation by two four-legged robots with implicit communication. Robotics and Autonomous Systems 1999. pp.13{19.

[12] Saranli U., Buehler M., Koditschek D.E. (2001) Rhex: A simple and highly mobile hexapod robot. *International Journal of Robotics Research* 20:616{ 631

[13] Ben-Tzvi P., Goldenberg A.A., Zu J.W. (2010) Articulated hybrid mo- bile robot mechanism with compounded mobility and manipulation and on- board wireless sensor/actuator control interfaces. In: Mechatronics 20(6), pp 627 639,

[14] Krid M., Ben Amar F. (2011) A dynamic based path tracking controller for a fast rover with independent steering and drive. in Proc. *International Conference on Climbing and Walking Robots*, CLAWAR'11, Paris, France, Septembre 2011.

[15] WONG J.Y. (2008) Theory of ground vehicles, fourth edition edn

[16] http://www.segway.com/

[17] Kim D., Hong H., Kim H.S., Kim J. (2012) Optimal design and kinetic anal-ysis of a stair-climbing mobile robot with rocker-bogie mechanism. Mecha- nism and Machine Theory 50(0), pp 90 { 108.

[18] Hashimoto M., Oba F., Eguchi T. (1993) Dynamic control approach for motion coordination of multiple wheeled mobile robots transporting a single object. In: Intelligent Robots and Systems '93, IROS '93. Proceedings of the 1993 IEEE/RSJ International Conference on, vol 3, pp 1944{1951.

[19] Kosuge K., Oosumi T. (1996) Decentralized control of multiple robots han- dling an object. In: Intelligent Robots and Systems '96, IROS 96, Proceed- ings of the 1996 IEEE/RSJ International Conference on, vol 1, pp 318{323.

[20] Kurabayashi D., Sasaki J., Aiyama Y. (1996) Cooperative transport with regrasping of torque-limited mobile robots. In: Intelligent Robots and Systems '96, IROS 96, Proceedings of the 1996 IEEE/RSJ International Conference on, vol 1, pp 304{309.

[21] Christopher M Holland PBO Constantine Marmaras (Jan 17, 2013) Remote controlled load transport system, Pub. No.: US 2013/0017047 A1.

[22] Wobben A. Transport vehicle for oversized loads. Patent EP1465789 B1, (Apr 16, 2008).

[23] Chebab, Z.E.: Optimization of a climbing process. Master's thesis 2013, Pierre and Marie Curie University, UPMC, Paris VI.

[24] Ishihara, H., Kuroi, K.: A four-leg locomotion robot for heavy load trans- portation. IEEE/RSJ International Conference Intelligent Robots and Sys- tems, IROS 2006. pp. 5731{5736.

[25] Thomas V. Edgar, M.A.U., Hamann, J.C.: The static stability factor a dynamic introduction to engineering. In: American Society for Engineering Education Annual Conference and Exposition, 2005.

[26] Papadopoulos, E., Rey, D.: A new measure of tipover stability margin for mobile manipulators. IEEE International Conference Robotics and Automa- tion, 1996. on, vol. 4, pp. 3111{3116.

[27] National Highway Tra_c Safty Administration, National Technical Infor- mation Service, Spring_eld, Virginia 22161: Trends in the Static Stability Factor of Passenger Cars, Light Trucks, and Vans, 2005.
[28] Sugano, S., Huang, Q., Kato, I.: Stability criteria in controlling mobile robotic systems. *IEEE/RSJ International Conference Intelligent Robots and Systems*, IROS 1993. on, vol. 2, pp.832{838.
[29] Pereira, F.G., de Sa, F.B., Ferreira, D.B., Vassallo, R.F.: Object trans- portation task by a human and a mobile robot. *IEEE International Conference Industrial Technology*, ICIT 2010. pp. 1445{1450.
[30] Wyrobek, K., Berger, E., Van der Loos, H., Salisbury, J.: Towards a per- sonal robotics development platform: Rationale and design of an intrinsically safe personal robot. *IEEE International Conference Robotics and Automation*, ICRA 2008. pp. 2165{2170.
[31] Hamner, B., Koterba, S., Shi, J., Simmons, R., Singh, S.: An autonomous mobile manipulator for assembly tasks. Autonomous Robots 2010. pp.131{ 149.
[32] Loh, C.C., Traechtler, A.: Cooperative transportation of aload using non- holonomic mobile robots. International Symposium on Robotics and Intel- ligent Sensors, IRIS 2012. pp.860 { 866.
[33] Bouton, N., Lenain, R., Thuilot, B., Martinet, P.: A rollover indicator based on a tire sti_ness backstepping observer: Application to an all-terrain vehicle. *IEEE/RSJ International Conference Intelligent Robots and Sys-tems*, IROS 2008. pp. 2726{2731.
[34] Safar, M., Watanabe, K., Maeyama, S., Nagai, I.: A study of tipping stabil- ity for omnidirectional mobile robot with active dual-wheel caster assemblies. Arti_cial Life and Robotics, 2012. pp.145{151 (2012).
[35] Ali, S., Moosavian, A., Alipour, K.: Stability evaluation of mobile robotic systems using moment-height measure. IEEE Conference Robotics, Automa- tion and Mechatronics, 2006. pp. 1{6.
[36] Fauroux, J.C., Chapelle, F., Bouzgarrou, B.: Openwheel i3r-a new archi- tecture for clearance performance. Proc. of ROBOTICS 2010, *International Workshop for Environment/Agriculture*.
[37] Fauroux, J.C., Bouzgarrou, B. and Krid M., Robot unit for transporting long loads , pn. WO2015128594 A1, Sep 3. 2015, IFMA.